

# Large Nonlinear Absorption in Coated Ag<sub>2</sub>S/CdS Nanoparticles by Inverse Microemulsion

M. Y. Han,<sup>\*,†</sup> W. Huang, C. H. Chew, and L. M. Gan\*

Department of Chemistry and Institute of Materials Research & Engineering, National University of Singapore, Singapore 119260

X. J. Zhang and W. Ji\*

Department of Physics, National University of Singapore, Singapore 119260

Received: September 3, 1997; In Final Form: November 24, 1997

A modified inverse microemulsion technique was used to synthesize coated Ag<sub>2</sub>S/CdS nanocomposites of ~10 nm in diameter. Their nonlinear absorption was observed with picosecond and nanosecond laser radiation of 532-nm wavelength. The nonlinear absorption in the Ag<sub>2</sub>S/CdS nanocomposites was enhanced, in comparison with the CdS nanoparticles, due to free-carrier absorption. In addition, the relaxation times of photoexcited free carriers in the Ag<sub>2</sub>S/CdS nanocomposites were also determined to be a few nanoseconds.

## Introduction

Information processing by using optical technology has created a great need for novel materials with large nonlinear optical (NLO) response and short response time.<sup>1</sup> NLO materials have also received considerable attention as a result of growing demand for the protection of optical sensors.<sup>2</sup> The most common approach is to synthesize new materials possessing the desirable NLO attributes as inherent properties. An alternative approach is to fabricate composites of a few nanometers in size for improving their NLO properties. In this paper, we report the observation of strong nonlinear absorption in a new nanometer-sized system synthesized by a microemulsion method.

Optical nonlinearities in bulk semiconductors and their potential applications have been extensively investigated.<sup>3</sup> The reduction in the dimensionality of semiconductor systems from bulk to nanoscale can enhance their nonlinearities due to the quantum size effect and other mesoscopic phenomena of nanoparticles.<sup>4,5</sup> In recent years, there has been intense research on the NLO properties of nanometer-sized semiconductors and fabrication techniques for these small particles. Semiconductor nanoparticles embedded in glass (commercially referred to as color filters) may be synthesized by a method of cosputtering and thermal annealing, and their NLO properties have been characterized.<sup>6–8</sup> Semiconductor microcrystallites can also be produced by several techniques such as direct chemical reaction in aqueous or organic solution.<sup>4</sup> Recently, a microemulsion technique has been developed to prepare semiconductor nanocomposites such as ZnS/CdSe, ZnSe/CdSe, or ZnS/CdS in a core-shell structure.<sup>9–11</sup> Both absorption and photoluminescence spectra of these quantum particles have been reported.<sup>9,11</sup> However, the NLO properties of such interesting systems have not been scrutinized. Here we present experimental results of the nonlinear absorption in coated Ag<sub>2</sub>S/CdS nanocomposites prepared by a modified microemulsion technique. To the best of our knowledge, this is the first investigation on the NLO

properties of semiconductor nanocomposites in stable, transparent microemulsions.

## Experimental Section

We prepared our nanocomposites in microemulsions at room temperature with the following materials. Sodium bis(2-ethylhexyl)sulfosuccinate (Na-AOT) purchased from Fluka was used without further purification. CdBr<sub>2</sub> (99%, Fluka), (NH<sub>4</sub>)<sub>2</sub>S (20 wt % in aqueous solution, Merck), AgNO<sub>3</sub> (99.8%, Merck), and heptane (A. R. Grade, J. T. Baker) were all used as received. Water was purified by a Millipore system (Milli-Q).

The clear region of the water-in-oil microemulsion was determined visually by titrating the aqueous solution to a Na-AOT–heptane solution in a screw-capped tube. It was thoroughly mixed with a vortex mixer. The clear–turbid boundaries were established from systematic titrations. The transparent region was also identified for (NH<sub>4</sub>)<sub>2</sub>S or CdBr<sub>2</sub> in the microemulsion. In Figure 1, the shaded areas show the microemulsion regions of two types of inverse microemulsions (designated as MA and MB, respectively). MA consisted of an aqueous solution of 0.1 M (NH<sub>4</sub>)<sub>2</sub>S, while MB contained an aqueous solution of 0.1 M CdBr<sub>2</sub>. The common components used for both MA and MB were Na-AOT and heptane. At a given weight ratio of Na-AOT to heptane ( $w = 18/82$ ), a straight line was drawn from the apex of the aqueous solution as shown in Figure 1. One can then prepare a reaction microemulsion by mixing equal amounts of MA and MB within the microemulsion regions. Thus the stability of the reaction microemulsion should be least disturbed because the  $w$  value remains unchanged after mixing MA and MB.

The preparation of coated Ag<sub>2</sub>S/CdS small particles involved two processes, namely (1) the formation of CdS cores and (2) the coating with Ag<sub>2</sub>S. In the first process, MA and MB were prepared separately. The two microemulsions with equal weight were then mixed by vigorously stirring. A light yellow transparent microemulsion solution of the CdS cores was formed immediately. After a few minutes of mixing the microemulsions, the coating process took place with adding an aqueous solution of 0.1 M AgNO<sub>3</sub>. This resulted in the formation of

\* To whom correspondence should be addressed.

† E-mail: chmhanmy@leonis.nus.sg. Fax: 65-7791691.

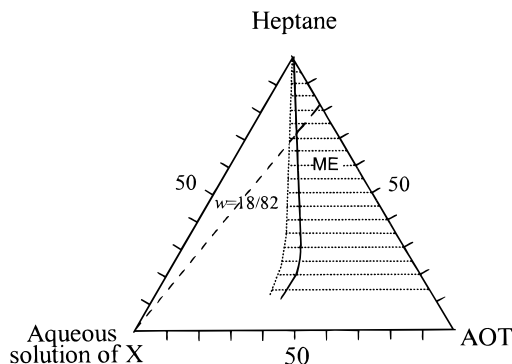


**Figure 1.** Phase diagrams of inverse microemulsions at 30 °C. Microemulsion A (—), X = 0.1 M (NH<sub>4</sub>)<sub>2</sub>S aqueous solution. Microemulsion B (---), X = 0.1 M CdBr<sub>2</sub> aqueous solution. The long dashed line is drawn at the weight ratio of Na-AOT to heptane,  $w = 18/82$ .

**TABLE 1: Compositions of the Mixed Microemulsions<sup>a</sup>**

mixed microemulsions <sup>b</sup>	aqueous solution A for MA (wt %)	aqueous solution B for MB (wt %)	the third component <sup>c</sup>
CdS (1:1)	4% (NH <sub>4</sub> ) <sub>2</sub> S (0.1 M)	4% CdBr <sub>2</sub> (0.1 M)	
CdS (2:1)	4% (NH <sub>4</sub> ) <sub>2</sub> S (0.1 M)	8% CdBr <sub>2</sub> (0.1 M)	
CdS (3:1)	4% (NH <sub>4</sub> ) <sub>2</sub> S (0.1 M)	12% CdBr <sub>2</sub> (0.1 M)	
CdS (4:1)	4% (NH <sub>4</sub> ) <sub>2</sub> S (0.1 M)	16% CdBr <sub>2</sub> (0.1 M)	
Ag <sub>2</sub> S/CdS (1:1)	4% (NH <sub>4</sub> ) <sub>2</sub> S (0.1 M)	4% CdBr <sub>2</sub> (0.1 M)	AgNO <sub>3</sub> (0.1 M)
Ag <sub>2</sub> S/CdS (2:1)	4% (NH <sub>4</sub> ) <sub>2</sub> S (0.1 M)	8% CdBr <sub>2</sub> (0.1 M)	AgNO <sub>3</sub> (0.1 M)
Ag <sub>2</sub> S/CdS (3:1)	4% (NH <sub>4</sub> ) <sub>2</sub> S (0.1 M)	12% CdBr <sub>2</sub> (0.1 M)	AgNO <sub>3</sub> (0.1 M)
Ag <sub>2</sub> S/CdS (4:1)	4% (NH <sub>4</sub> ) <sub>2</sub> S (0.1 M)	16% CdBr <sub>2</sub> (0.1 M)	AgNO <sub>3</sub> (0.1 M)

<sup>a</sup> All samples were prepared in microemulsions containing different aqueous solution at a fixed weight ratio of 18/82 for Na-AOT/heptane.

<sup>b</sup> The ratios denote Cd<sup>2+</sup>/S<sup>2-</sup> in a mixed microemulsion. The amount of AgNO<sub>3</sub> aqueous solution used was twice the amount of solution A.

<sup>c</sup> Same amounts of AgNO<sub>3</sub> aqueous solutions were used in preparing the nanocomposites.

greenish yellow coated Ag<sub>2</sub>S/CdS (1:1) nanocomposites via the displacement reaction  $2\text{Ag}^+ + \text{CdS(s)} \rightarrow \text{Cd}^{2+} + \text{Ag}_2\text{S(s)}$ . The detailed constituents and compositions for the synthesis are summarized in Table 1. The TEM results show that the Ag<sub>2</sub>S/CdS (1:1) particles have a diameter of  $\sim 10$  nm.

The particle solutions were placed in quartz cuvettes for optical measurements. The nonlinear absorption in our nanoparticles and nanocomposites was measured with linearly polarized pulses (25-ps and 7-ns fwhm) from two frequency-doubled Nd:YAG lasers: the first was mode-locked and Q-switched, and the second was Q-switched only. The pulses had a nearly Gaussian spatial profile and were focused onto a 1-mm-thick cuvette containing the sample with a 25- $\mu\text{m}$  beam waist ( $H\text{We}^{-2}\text{M}$ ) at the focus. Both the incident and the transmitted pulses were monitored simultaneously by two energy probes (Laser Precision, RjP-735), which sent the signals to a computer. The energy of the incident pulses was controlled by inserting a set of neutral density filters in front of the laser. The nonlinear absorption of the sample was examined by moving the sample along the direction of the incident beam with respect to the focal point, similar to a standard open-aperture Z-scan technique.<sup>12</sup>

## Results and Discussion

The AgNO<sub>3</sub> aqueous solution has been chosen as the third individual component for coating. The addition of AgNO<sub>3</sub> aqueous solution to the microemulsion system enables Ag<sup>+</sup> ions to diffuse into the microemulsion droplets to form semiconductor nanoparticles. Different ratios in the brackets denoted Cd/S in their corresponding mixed microemulsions. However, it is

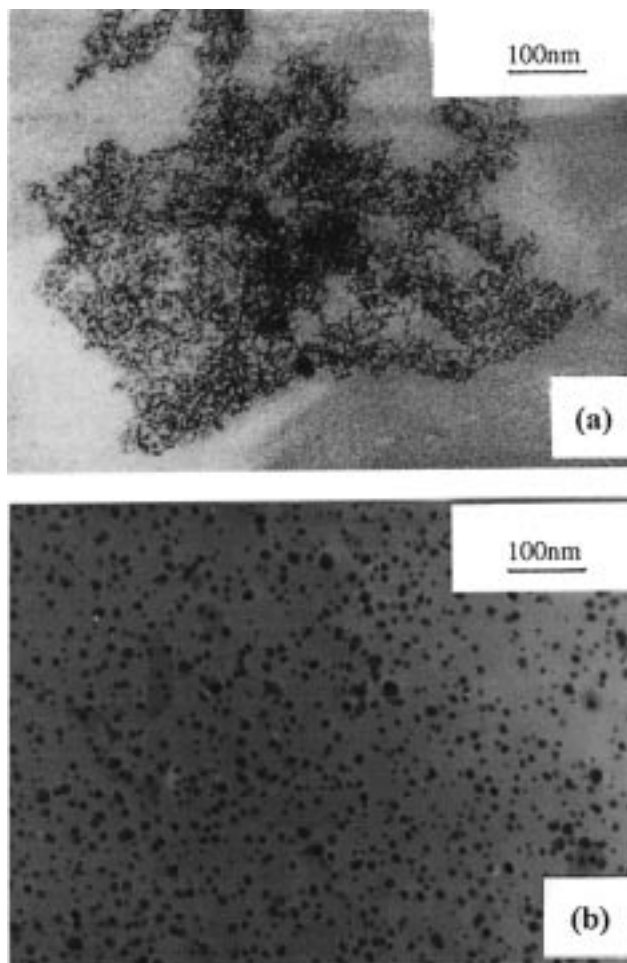


**Figure 2.** Transmission electron micrographs of the CdS (1:1) nanoparticles and Ag<sub>2</sub>S/CdS (1:1) nanocomposites in an inverse microemulsion.

difficult to identify the elements present in individual particles or small groups of particles because of a large amount of surfactant capped on the surface of those particles. The surfactant layer was thus required to be removed first by washing several times with water. The residual surfactant was then washed away with hexane. It was interesting that only three elements, cadmium, silver, and sulfur, were identified by means of EDX analysis in the resulting powder, which showed that Ag<sub>2</sub>S-coated CdS nanoparticles were formed. The similar and sole structures such as ZnSe/CdSe were reported in several references.<sup>13,14</sup> Figure 2 displays the TEM micrographs, which indicate an average diameter of 5 and 7 nm for the CdS cores and the Ag<sub>2</sub>S/CdS (1:1) nanocomposites, respectively. This also implies a core-shell structure. The Ag<sub>2</sub>S-coated CdS particles were prepared via the displacement reaction  $2\text{Ag}^+ + \text{CdS(s)} \rightarrow \text{Cd}^{2+} + \text{Ag}_2\text{S(s)}$ . The resulting compact Ag<sub>2</sub>S shell with small solubility product can prevent the Ag<sup>+</sup> ions outside of Ag<sub>2</sub>S shell from diffusing into the interface between the CdS core and Ag<sub>2</sub>S shell further. The formation of AgBr particles was hindered by the formation of Ag-AOT via the displacement reaction  $\text{Na-AOT} + \text{Ag}^+ \rightarrow \text{Na}^+ + \text{Ag-AOT}$  in the production of the nanoparticles. This phenomenon should arise from the lower dissociation ability of Ag-AOT as compared to Na-AOT and AgBr.

Figure 3 shows the UV-visible absorption spectra for CdS (1:1) and Ag<sub>2</sub>S/CdS (1:1) nanoparticles and nanocomposites in microemulsions. The absorption spectrum of the CdS particles possesses an exciton absorption peak at 410 nm, consistent with

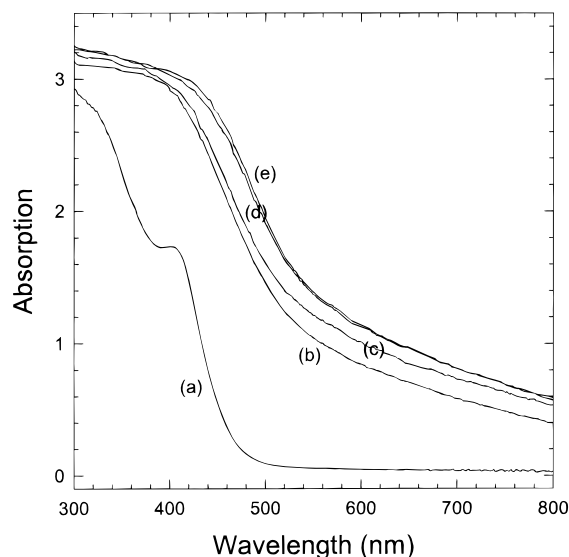


**Figure 3.** Absorption spectra of (a) CdS (1:1), (b) Ag<sub>2</sub>S/CdS (1:1), (c) Ag<sub>2</sub>S/CdS (2:1), (d) Ag<sub>2</sub>S/CdS (3:1), and (e) Ag<sub>2</sub>S/CdS (4:1) nanoparticles or nanocomposites in microemulsions. The optical length is 1 cm.

the previous observation.<sup>15</sup> For the Ag<sub>2</sub>S/CdS nanocomposites, it is expected that its absorption should result from the absorption of its two constituents: the Ag<sub>2</sub>S shell and CdS core. However, the absorption tail covering the entire visible spectral region is caused by the formation of Ag<sub>2</sub>S on the surface of the CdS core. The absorption spectra of Ag<sub>2</sub>S small particles have been examined by Motte et al., which shows an absorption tail in the wavelength ranging from 500 to 800 nm.<sup>16</sup>

For comparison reasons, we have measured the nonlinear absorption in the CdS nanoparticles.<sup>17,18</sup> Parts a and b of Figure 4 are the normalized transmittance of the CdS nanoparticles in the microemulsion with the 25-ps and 7-ns pulses, respectively. The two Z scans are obtained with the same fluence (1.8 J/cm<sup>2</sup>) but different irradiances (67 and 0.25 GW/cm<sup>2</sup>) due to the different pulse duration.<sup>19</sup> The observed nonlinear absorption results from two-photon absorption (TPA). The solid curves in Figure 4a,b are calculated by the standard Z-scan theory for the TPA.<sup>12</sup> From these best fits, we obtain a TPA coefficient of  $7.6 \times 10^{-11}$  cm/W or an imaginary third-order susceptibility,  $\text{Im } \chi^{(3)}$ , of  $2.9 \times 10^{-22}$  m<sup>2</sup>/V<sup>2</sup> for a volume fraction of  $\sim 10^{-4}$ , close to the data found for the Cd(Se,Te) nanoparticles in glass.<sup>8</sup> With the nanosecond laser pulses, the irradiance is less than 1 GW/cm<sup>2</sup>, and hence, the TPA is insignificant as shown by Figure 4b.

Parts c and d of Figure 4 show two examples of the Z-scan data obtained from the Ag<sub>2</sub>S/CdS (1:1) nanocomposites measured with the pulses of two durations. At a fluence of 1.4 J/cm<sup>2</sup>, the transmittance of the nanocomposites falls to 50% and 70% of the linear transmittance ( $\sim 70\%$ ) for the picosecond and nanosecond pulses, respectively. This is comparable to the nonlinear absorptive performance of C<sub>60</sub>, a benchmark optical limiter.<sup>20</sup> To investigate the composition dependence, we also recorded the Z scans of the Ag<sub>2</sub>S/CdS with various ratios of Cd<sup>2+</sup> to S<sup>2-</sup>. The strongest nonlinear absorption has been found in the composition ratios of 2:1 to 4:1. The observed nonlinear absorption is enhanced because of the introduction of the Ag<sub>2</sub>S shell. In this case, the nonlinear absorption is mainly contributed by an excited-state absorption process, in which electrons in the valence band are excited to intermediate energy states because of the linear absorption tail. These electrons and holes in the valence band then make transitions to higher energy states,

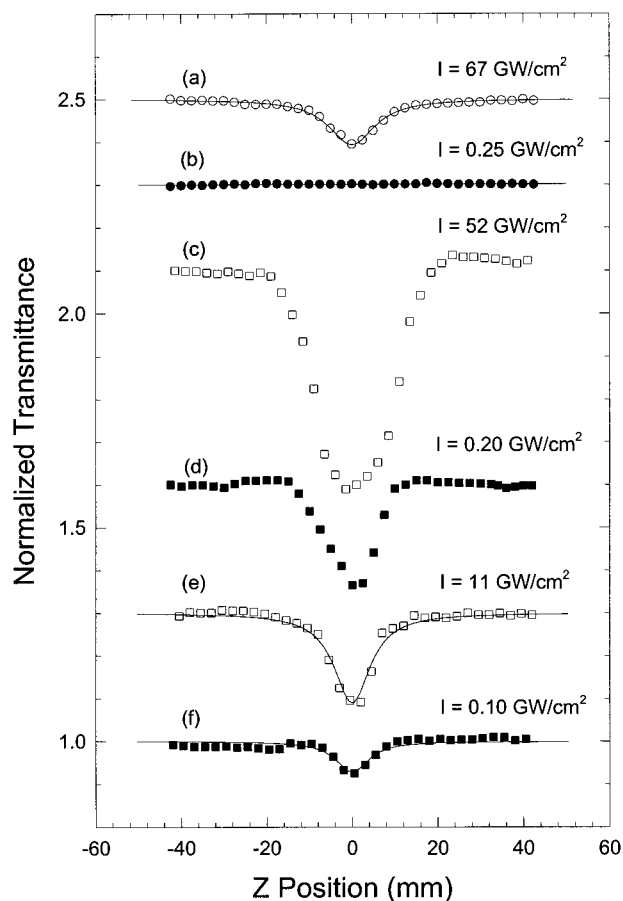


**Figure 4.** Measured normalized transmittance as a function of the sample position  $z$  for the CdS nanoparticles (the circles) and the Ag<sub>2</sub>S/CdS (1:1) nanocomposites (the squares). The data in a, c, and e were measured with the 25-ps laser pulses, while the data in b, d, and f were recorded with the 7-ns laser pulses. The laser wavelength is 532 nm, the pulse repetition rate is 10 Hz, and the optical path is 1 mm. The solid curves are the simulations described in the text. The data and curves in a, b, c, d, and e are vertically shifted by 1.5, 1.3, 1.1, 0.6, and 0.3, respectively, for presentation.

giving rise to the nonlinear absorption. Such a process is referred to as free-carrier absorption in bulk semiconductors or excited-state absorption in conjugated molecular systems.

To quantify the free-carrier absorption, we have conducted the Z scans at lower irradiances, as displayed in Figure 4e,f. The total absorption coefficient  $\alpha$  is described by  $\alpha = \alpha_0 + \sigma N$ , where  $\alpha_0$  is the linear absorption coefficient and  $\sigma$  and  $N$  are the absorption cross section and photoexcited carrier density, respectively. For the picosecond Z scans, the relaxation time of the excited carriers is assumed to be on the order of a few nanoseconds, and then the photoexcited carrier density may be estimated by  $dN/dt = \alpha_0 I / \hbar \omega$ , where  $I$  and  $\hbar \omega$  are the irradiance within the sample and the photon energy, respectively. By using this equation, the normalized transmittance as a function of the sample position  $z$  may be calculated numerically following an iteration method reported in ref 21. Note that all the parameters are known except for  $\sigma$ . Therefore it is extracted from the best fitting between the simulation and experimental data, as shown by the curve of Figure 4e. The extracted  $\sigma$  values for the Ag<sub>2</sub>S/CdS particles are listed in Table 2, which also includes the  $\sigma$  values for other nanocomposites by similar Z scans and analysis. With these  $\sigma$  values, one can estimate the free-carrier absorption to be at least 1 order of magnitude greater than the TPA in the CdS small particles, and thus the TPA can be neglected in our calculation.

**TABLE 2: Nonlinear Parameters for the Nanoparticles and Nanocomposites<sup>a</sup>**

sample	V	$\alpha_0$ (cm <sup>-1</sup> )	$\sigma$ ( $\times 10^{-18}$ cm <sup>2</sup> )	$\tau$ (ns)	$\beta$ ( $\times 10^{-11}$ cm/W)
CdS (1:1)	$\sim 10^{-4}$	0.49			7.6
Ag <sub>2</sub> S/CdS (1:1)	$\sim 10^{-4}$	3.8	4.2	0.59	
Ag <sub>2</sub> S/CdS (2:1)	$\sim 10^{-4}$	3.9	3.1	1.9	
Ag <sub>2</sub> S/CdS (3:1)	$\sim 10^{-4}$	4.0	5.0	3.3	
Ag <sub>2</sub> S/CdS (4:1)	$\sim 10^{-4}$	4.0	3.7	4.6	

<sup>a</sup> V (volume fraction) denotes the volume percentage of nanoparticles and nanocomposites in the microemulsion.  $\alpha_0$  is the linear absorption coefficient,  $\beta$  is the two-photon absorption (TPA),  $\sigma$  and  $\tau$  are the absorption cross section and relaxation time of the photoexcited carriers, respectively.

We also simulate the nanosecond Z scans for the Ag<sub>2</sub>S/CdS composite particles. In this case, the carrier relaxation effect has to be included, and the photoexcited carrier density is calculated by  $dN/dt = \alpha_0 I/\hbar\omega - N/\tau$ , where  $\tau$  is the relaxation time, the only unknown quantity. By fitting to the measured Z scans, the relaxation times can be deduced and are listed in Table 2; they are typically on the order of a few nanoseconds. The deduced lifetimes are much longer than 25 ps, justifying our treatment of the picosecond Z scans.

In summary, the large free-carrier absorption in the nanocomposites prepared by the microemulsion technique has been observed for the first time. The great potential of using the microemulsion method to synthesize nanocomposites lies in the fact that their constituent elements and particle sizes can readily be altered to optimize the desired NLO properties. Experiments designed to examine the influence of constituents and particle sizes are already under way.

## References and Notes

(1) Khoo, I. C.; Simoni, F.; Umeton, C. *Novel Optical Materials and Applications*; John Wiley & Sons: New York, 1997.

- (2) Perry, J. W.; Mansour, K.; Lee, I.-Y. S.; Wu, X.-L.; Bedworth, P. V.; Chen, C.-T.; Ng, D.; Marder, S. R.; Miles, P.; Wada, T.; Tian, M.; Sasabe, H. *Science* **1996**, 273, 1533 and references therein.
- (3) (a) Haug, H. *Optical Nonlinearities and Instabilities in Semiconductors*; Academic Press: Boston, 1988. (b) Born, W. E. *Ultrashort Processes in Condensed Matter*; Plenum Press: New York, 1993.
- (4) Henneberger, F.; Schmitt-Rink, S.; Göbel, E. O. *Optics of Semiconductor Nanostructures*; Akademie Verlag: Berlin, 1993.
- (5) Yoffe, A. D. *Adv. Phys.* **1993**, 42, 173.
- (6) Wang, Y. *Acc. Chem. Res.* **1991**, 24, 133.
- (7) Cotter, D.; Burt, M. G.; Manning, R. J. *Phys. Rev. Lett.* **1992**, 68, 1200.
- (8) Oak, S. M.; Bindra, K. S.; Chari, R.; Rustagi, K. C. *J. Opt. Soc. Am. B* **1993**, 10, 613.
- (9) Kortan, A. R.; Hull, R.; Opila, R. L.; Bawendi, M. G.; Steigerwald, M. L.; Carroll, P. J.; Brus, L. E. *J. Am. Chem. Soc.* **1990**, 112, 1327.
- (10) Hoener, C. F.; Allan, K. A.; Bard, A. J.; Campion, A.; Fox, M. A.; Mallouk, T. E.; Webber, S. E.; White, J. M. *J. Phys. Chem.* **1992**, 96, 3812.
- (11) Qi, L.; Ma, J.; Cheng, H.; Zhao, Z. *Colloid Surface A* **1996**, 111, 195.
- (12) Sheik-Bahae, M.; Said, A. A.; Wei, T. H.; Hagan, D. J.; Van Stryland, E. W. *IEEE J. Quantum Electron.* **1990**, 26, 760.
- (13) Peng, X. G.; Schlamp, M. C.; Kadavanich, A. V.; Alivisatos, A. P. *J. Am. Chem. Soc.*, in press.
- (14) Danek, M.; Jensen, K. F.; Murry, C. B.; Bawendi, M. G. *Chem. Mater.* **1996**, 8, 173.
- (15) Vossmeier, T.; Katsikas, L.; Giersig, M.; Popovic, I. G.; Diesner, K.; Chemseddine, A.; Eychmüller, A.; Weller, H. *J. Phys. Chem.* **1994**, 98, 7665.
- (16) Motte, L.; Billoudet, F.; Pileni, M. P. *J. Phys. Chem.* **1995**, 99, 16425.
- (17) For comparison reasons, we report only the nonlinear absorption of CdS nanoparticles in this paper because there was no observable nonlinear refraction in the nanocomposites.
- (18) (a) Schwerzel, R. E.; Kurmer, J. P.; Wood, V. E.; Jenkins, J. A. *Nonlinear Optical Properties of Organic Materials III, SPIE Proceedings, San Diego* **1990**, 1337, 132. (b) Schwerzel, R. E.; Spahr, K. B. *Abstr. Pap. Am. Chem. Soc.* **1994**, 208, 31.
- (19) Here the fluence and the irradiance are defined as the maximum fluence or irradiance on the optic axis at the focus within the sample.
- (20) McLean, D. G.; Sutherland, R. L.; Brant, M. C.; Brandelik, D. M.; Fleitz, P. A.; Pottenger, T. *Opt. Lett.* **1993**, 18, 858.
- (21) Tseng, K. Y.; Wong, K. S.; Wong, G. K. L. *Opt. Lett.* **1996**, 21, 180.